



New electrochemical method for separation of the iodine-131 radiopharmaceutical produced from uranium-235 fission

Thayna Campeol Marinho¹ · Elita Fontenele Urano de Carvalho¹ · Valéria Cristina Fernandes² · Artur José Santos Mascarenhas² · Elisabete Inácio Santiago¹

Received: 30 June 2024 / Revised: 15 August 2024 / Accepted: 29 August 2024
© The Author(s), under exclusive licence to Springer-Verlag GmbH Germany, part of Springer Nature 2024

Abstract

An alternative method based on electrochemical techniques for separation and purification of iodine in the presence of ruthenium, molybdenum, and tellurium, which are some elements resultants from uranium fission reaction, is proposed. For this, all elements were electrochemically characterized using the cyclic voltammetry technique. All the characterization and separation were performed using different parameters, such as temperature, pH, concentration, and potential, aiming to determine the optimized operation conditions to achieve the highest separation yield. The highest iodine yields were observed in acidic medium, at 298 and 313 K, and in lower iodine concentrations, which resulted in a separation rate of 45%. On the other hand, the iodine separation in basic medium resulted in very poor yields, indicating that the separation is not efficient in $\text{pH} > 8$.

Keywords Radiopharmaceutical · Iodine-131 · Electrochemical separation · Cyclic voltammetry

Introduction

Radiopharmaceuticals are radioisotopes related to biological molecules for the purpose of diagnosing and treating diseases [1]. The iodine-131 is an important radiopharmaceutical mainly used in thyroid diseases, but it can also be used for diagnosing abnormal liver function, renal blood flow, and urinary tract obstruction. Iodine is a beta

emitter and has a physical half-life of 8.04 days and biological half-life of 120 days in thyroid. It was used for the first time about 80 years ago and, since then, iodine-131 has been widely used in thyroid cancer treatment, being applied after thyroidectomy surgery, and aiming to remove thyroid tissue that may have remained after surgery [2–4].

The iodine-131 can be obtained from uranium-235 fission in a nuclear reactor. This reaction has an iodine-131 fission yield of 2.84% [5] and could originate several different elements as molybdenum-99, ruthenium-103, tellurium-132, and others [6, 7], which need to be separated from iodine-131 to fulfill the requirement to be a radiopharmaceutical. To solve this problem, researchers have proposed some separation and purification methods, so that the separated iodide-131 reaches the requirements for administration as a radiopharmaceutical in an effective and safe manner. The most of studies have employed adsorbents and sorbents to separate, extract, and purify the iodine-131 [8–11]. Iodine-131 can also be produced by other ways, such as from TeO_2 irradiation [12, 13], which also leads to tellurium-decay interferences.

Treushchenko et al. [14] have reported a method to remove radioactive gaseous iodine based on the ability of magnesium oxide (MgO) in reacting with iodine to form rocklike structures. The authors obtained high iodine

✉ Thayna Campeol Marinho
thayna.campeol@estudante.uam.es

✉ Elisabete Inácio Santiago
elisabete.santiago@usp.br

Elita Fontenele Urano de Carvalho
elitaucf@ipen.br

Valéria Cristina Fernandes
valcrisfer@ufba.br

Artur José Santos Mascarenhas
artur@ufba.br

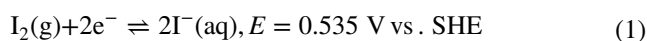
¹ Nuclear and Energy Research Institute, Avenida Professor Lineu Prestes, São Paulo, SP 224205508000, Brazil

² Physical Chemistry Department, Institute of Chemistry, Federal University of Bahia, Rua Barão de Jeremoabo, Campus Universitário de Ondina147, Bahia, Salvador 40170-115, Brazil

absorption (80–90%), after using multi-step removal processes alternating MgO absorption and the addition of hydrogen peroxide. In addition, Yang et al. [15] used silver oxide (Ag₂O) nanocrystals deposited on the external surface of sodium tri-titanate nanotubes (T3NT) and nanofibers (T3NF) to remove radioactive iodine anions from wastewater, and the result was an efficient capturing of I⁻ ions and easy separation of the adsorbent from a fluid. The use of a modified wet distillation apparatus for iodine purification changing parameters like temperature, process time, and catalyst effects is described by Damasceno et al. [16]. As a result, an iodine-131 recovery yield of ca. 50% is reported. Del Rio et al. [17] used a metal–organic framework silver-functionalized as sorbent to remove iodine from wastewaters, obtained 86 to 100% of extraction, with the limitation of using the sorbent to a maximum of three times without losing performance.

Considering the high potential for use of molybdenum-99 as a radiopharmaceutical for the generation of technetium-99m, which is widely used for diagnosing diseases, the removal of iodine is also important for the separation and purification of molybdenum-99 [6, 7, 16, 18].

This work presents an alternative for selective separation of the iodine (in iodide form, I⁻) based on its ability in reacting electrochemically to form molecular iodine (I₂, see Eq. (1)) in distinct potential than that applied for usual interferents produced from uranium-235 fission, such as ruthenium, molybdenum, and tellurium. Thus, experiments were performed under different experimental conditions, such as pH, temperature, and concentration, as well as two different electrochemical methods, i.e., chronoamperometry (potential step) and square wave, aiming to obtain the most efficient separation yield in the absence or presence of such interferents.



Material and methods

All the experiments were performed in a three-electrodes cell (Fig. 1). As working electrode (WE) was used a 1 cm² platinum grid, the counter electrode (CE) was a platinum wire, and the reference electrode (RE) was a silver/silver chloride (Ag/AgCl). A nitrogen bubbler was used to purge the solution, creating an inert atmosphere to drag the gaseous I₂ formed by the redox reaction to the container. This container, which served as collector to I₂, was partially filled with a potassium hydroxide solution (1 mol L⁻¹), promoting the conversion of I₂ into I⁻.

The reactants used were potassium iodide (Alphatec, 99 wt% min), ammonium molybdate (Synth, 81–83 wt%

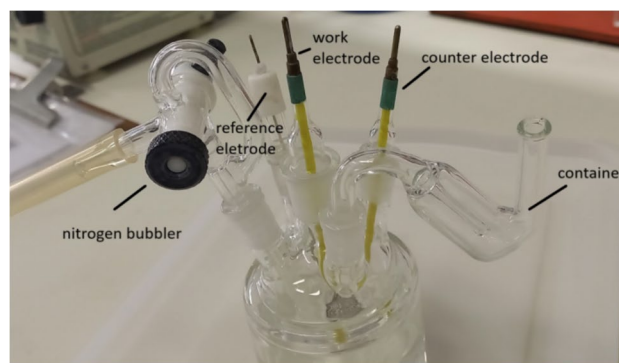


Fig. 1 Electrochemical cell used in all the experiments

MoO₃), tellurium dioxide (Sigma-Aldrich, 99 w% min), ruthenium (III) chloride (Sigma-Aldrich, 99.9 wt%), acetate buffer pH 8 and pH 5 (Neon), hydrochloric acid (Éxodo Científica, AR grade), potassium hydroxide (Éxodo científica, AR grade), and sulfonitric mixed acid (used for cleaning the electrode surface).

It is worth mentioning that all experiments were carried out with regular chemicals, in which no radioactive reactant was tested. In addition, a conventional three-electrodes cell was used in the experiments, which due to the fragile construction is prone to leak. Due to this reason, it was not possible to perform an accurate statistical separation analysis.

Determination of the electrochemically active surface area (ECSA)

The ECSA was estimated using the integration of the hydrogen underpotential deposition (H_{UPD}) from the cyclic voltammogram of buffer solution (pH 5) at 298 K to obtain the surface specific charge (Q_{spec}), followed by the conversion using a conversion factor of 210 μC cm⁻² [19, 20], according to the Eq. (2).

$$\text{ECSA} = \frac{Q_{\text{spec}}}{210 \mu\text{C}\cdot\text{cm}^{-2}} \quad (2)$$

Electrochemical characterization

The electrochemical characterization was an important part of this research because it aids to define the best iodine separation parameters. For this purpose, solutions of 0.001 mol L⁻¹, 0.005 mol L⁻¹, and 0.010 mol L⁻¹ concentration were prepared using iodide potassium, ammonium molybdate, tellurium dioxide, and ruthenium (III) chloride. Each compound was diluted separately in 20 mL of the adequate acetate buffer (pH 8 or pH 5), which acts as the electrolyte.

On the other hand, solutions containing all the elements simultaneously were prepared in both pH to study possible interactions between the elements.

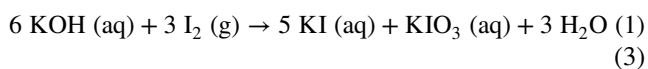
All electrochemical measurements were carried out using a Metrohm potentiostat/galvanostat, model PGSTAT128N, ranging from -1.0 to 1.0 V in a scan rate of 0.2 V/s, 10 cycles of each voltammogram were performed, and in most of the experiments the second cycle were plotted. The cell temperature was kept constant at 298 K, 313 K, or 333 K by using a thermostatic bath. The buffer acetate values were subtracted from current values obtained with the species (I, Mo, Te, and Ru) in order to obtain the voltammograms presented in this article.

A sulfonitric mixed acid was applied to clean the electrode surface after the experiments. The electrode was immersed in the solution for 15 min, followed by exhaustively washing with ultrapure water.

Iodine electrochemical separation

The separations were carried out in solutions containing iodine, in concentrations of 0.001 mol.L⁻¹, 0.005 mol L⁻¹, and 0.010 mol L⁻¹ in acid and basic electrolyte, at 298 K, 313 K, and 333 K, in the presence of all possible interferent elements considered in this study. For these experiments, the technique used was chronoamperometry, using a potential of 0.81 V vs. Ag/AgCl electrode, chosen from the voltammetry experiments. The experiments were conducted in two different ways: (i) single potential step, consisted of applying 50 mV for 600 s, 0.81 V for 4200 s and then 50 mV for 600 s; (ii) square wave, consisted of applying 50 mV for 300 s and 0.81 V for 600 s, intercalated up to 0.81 V for the total duration of 4200 s.

To capture the iodine coming from the redox reaction, the container was filled with a potassium hydroxide solution at 0.1 mol L⁻¹ concentration, which reacts with gaseous I₂ to produce in I⁻ and IO₃⁻ in aqueous solution, according to Eq. (3).



Iodide quantification

The quantification of the captured iodide was done using a direct amperometry technique. Initially, measurements were performed with standard solutions of concentrations 0.0005 mol L⁻¹, 0.001 mol L⁻¹, 0.005 mol L⁻¹, and 0.007 mol L⁻¹ of aqueous solutions of KI, using acid solutions of KCl as supporting electrolyte, which was obtained by adding 8 mL of hydrochloric acid 0.25 mol L⁻¹ and 10 mL of potassium hydroxide 0.1 mol L⁻¹. This solution was placed in the electrochemical cell and a potential of 0.84 V was applied for 20 s under constant agitation by

bubbling N₂ gas. After each experiment, the current value obtained was plotted in a graph of concentration vs current and a fitting analysis was performed to determine the calibration curve. After the calibration curve was built, 10 mL of the solution of iodine captured in KOH was added in 18 mL of the electrolyte previously used (10 mL KOH 0.1 mol L⁻¹ + 8 mL HCl 0.25 mol L⁻¹) and submitted to the same previous conditions to obtain concentrations values.

The calculation for the yield was carried out considering the amount of iodine before separation and after separation and dilution factors used during the procedure.

Results and discussions

Electrochemical characterization

To achieve iodine separation through its oxidation reaction, the parameters that could influence the process—temperature, pH, and species concentration—were studied using cyclic voltammetry technique. Molybdenum, tellurium, ruthenium, and iodine species were studied in separated solutions and in the same solution.

The electrode active surface area was calculated using Eq. (2), and it was obtained a value of 4.69 cm², from a Q_{spec} of 9.85E^{-4} C.

Iodide voltammetry

Figure 1 shows the cyclic voltammetry at pH 5, 298 K (A), 313 K (B), and 333 K (C) of iodide concentrations of 0.01 , 0.005 , and 0.001 mol.L⁻¹. The voltammograms obtained were quite stable, unchanging through the 10 cycles of the experiment. Well defined anodic peak potentials (E_{ap}) were readily identified in the voltammograms, especially at 298 K, this definition decrease with the increase in temperature.

The E_{ap} values at 298 K correspond to 0.813 V vs. Ag/AgCl to 0.01 mol L⁻¹, 0.710 V vs. Ag/AgCl to 0.005 mol L⁻¹ and 0.700 vs. Ag/AgCl to 0.001 mol L⁻¹. The peak-to-peak separation (ΔE_{p}) was calculated to provide information about the reversibility of the reaction. The values obtained, at scan rate of 20 mV s⁻¹ and 298 K, were 0.684 V to 0.01 mol L⁻¹, 0.432 V to 0.005 mol L⁻¹, and 0.322 V to 0.001 mol L⁻¹. For a one-electron redox couple, it was considered ΔE_{p} larger than 57 mV as a quasi-reversible reaction [21], as obtained at 0.01 mol L⁻¹. On the other hand, values smaller than 57 mV were obtained at 0.005 mol L⁻¹ and 0.001 mol L⁻¹, indicating a possible reversible kinetics.

At 313 K the E_{ap} of 0.01 mol L⁻¹ and 0.005 mol L⁻¹ potassium iodide were identified as 0.806 V and 0.798 V vs. Ag/AgCl, respectively. At 0.001 mol L⁻¹ it was not possible to identify the peaks due to the flattening of the

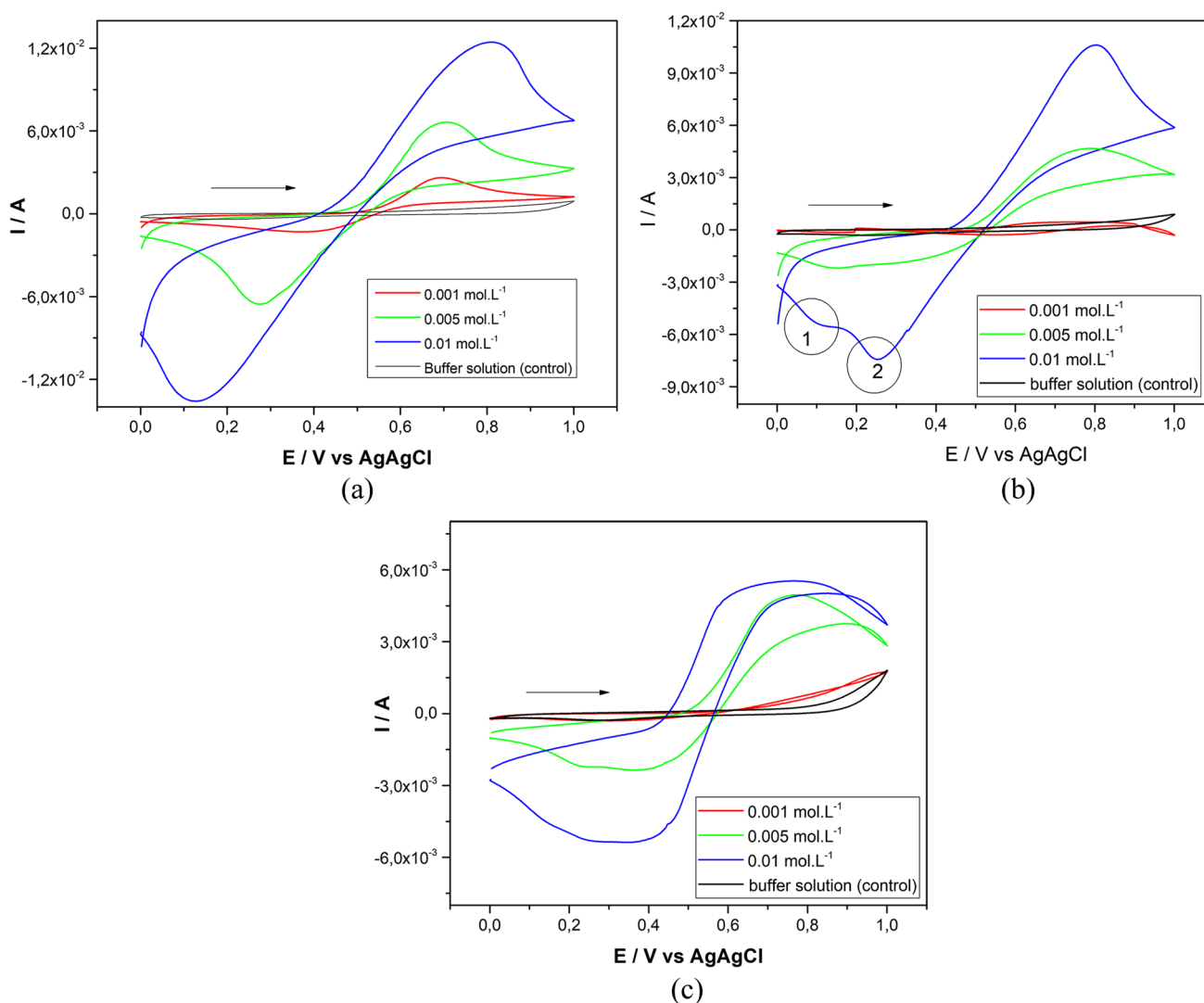


Fig. 2 Cyclic voltammograms of potassium iodide at 298 K (a), 313 K (b), and 333 K (c) in 0.001, 0.005, and 0.010 mol L⁻¹ acidic medium (pH=5)

voltammogram. The ΔE_p values of 0.552 V to 0.01 mol L⁻¹ and 0.637 V to 0.005 mol L⁻¹ indicate a reversible and quasi-reversible reaction, respectively. It was observed, at 0.01 mol L⁻¹ (indicated in Fig. 2b as 1 and 2), the presence of two anodic peaks, indicating the possibility of more than one redox process occurring at same time.

At 333 K, an increase in the velocity of the reaction leads to a flattening in the peaks, which difficulties the identification of the E_{ap} . The E_{ap} obtained to 0.01 mol L⁻¹ and 0.005 mol L⁻¹ were 0.835 and 0.796 V vs. Ag/AgCl, respectively, as occurred at 313 K, it was not possible to identify the values at 0.001 mol L⁻¹. The calculated ΔE_p resulted in 0.512 V to 0.01 mol L⁻¹ and 0.459 V to 0.005 mol L⁻¹, indicating reversible reactions.

According to the obtained E_{ap} values, it was possible to observe that, at 0.01 mol L⁻¹, the current reaches a

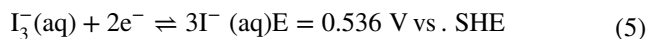
maximum at about 0.8 V vs. Ag/AgCl, while at 0.005 mol L⁻¹, it corresponds to about 0.70 V vs. Ag/AgCl, especially at 298 K. These values were consistent with the standard iodine oxidation reaction potential (0.535 vs. SHE) (Eq. (1)) and indicates the occurrence of the iodine oxidation reaction.

Nonetheless, when iodine in solution interacts with the iodide, a triiodide specie is formed (Eq. (4)). This is a secondary and undesirable reaction that could interfere in the voltammograms results once could suffer oxidation at 0.536 V vs. SHE (Eq. (5)), resulting in its conversion back to iodide. Consequently, the voltammograms could indicate more than one redox process occurring at same time, as observed at 313 K and 0.01 mol L⁻¹. Additionally, the presence of this specie hinders the iodine separation because it increases its solubility, favoring its permanence in the solution.

Triiodide formation reaction:



Triiodide oxidation reaction:



All voltammograms in the acid solution have presented peak current values that increase with the concentration of the potassium iodide solution, which is consistent with Faraday's 1st Law. Besides, the E_{ap} values have a small shift to more positive potentials as the solution becomes more concentrated. Comparing the voltammograms obtained at 298 K and 313 K, the redox processes occurring at more negative potentials are quite different, but there were no significant changes in the region where the iodide oxidation occurs (Fig. 2a, b).

At 333 K (Fig. 2c), a decrease in the current density can be observed when compared to lower temperatures. Additionally, the redox process loses definition in lower concentrations. At this temperature, redox iodine reaction occurs at higher reaction rate, and iodine tends to remain in the form of vapor. These factors shift the equilibrium (Eq. (4)), according to Le Chatelier's principle, to form a greater iodide amount. This would make it difficult the gaseous I_2 re-solubilization in the cell; in addition, the triiodide formation would be favored, besides the voltammetric curve loses definition regarding the evaluated redox processes.

The voltammograms obtained in basic medium differ significantly from those obtained in acidic medium. These results are shown in Supplementary Material just for comparison (Fig. S1). This type of electrochemical behavior (irreversible anodic processes [22], with poorly developed and undefined peaks) had already been reported previously [23]. These results indicate reactions with oxygen to form compounds as HIO , IO^- , and IO_3^- . The drops in current densities suggest low iodine formation and, consequently, difficulties in promoting the separation.

Electrochemical behavior in the presence of interferent elements

The interferent elements could be singly analyzed, some of which proved to be interfering depending on the pH value and temperature. The voltammograms of interferent elements are shown in Supplementary Material.

Ruthenium

Ruthenium is a very stable element in acidic medium; however, at elevated temperatures reacts with oxygen. The voltammogram of ruthenium at the temperature of 333 K and

concentration of 0.010 mol L^{-1} (Fig. S2) exhibits faradaic currents corresponding to the reduction from Ru^{3+} to Ru^{2+} ions, at 0.9 V vs. Ag/AgCl.

In alkaline solutions, ruthenium is solubilized and energetically oxidized, and it can form ruthenium(III) hydroxide ($\text{Ru}(\text{OH})_3$), which can easily be oxidized to ruthenium oxide ($\text{RuO}_2 \cdot 2\text{H}_2\text{O}$) or ruthenium(IV) hydroxide ($\text{Ru}(\text{OH})_4$) that could be reduced to elemental ruthenium [24, 25].

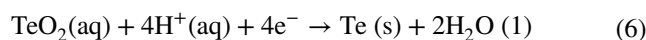
Molybdenum

Voltammograms of molybdenum in acidic medium (not shown) resulted in only capacitive current between potentials from 0 to 1.0 V, which suggest no interference in the separation of iodine. This finding is consistent with the literature [25], where molybdenum tends to passivate by forming insoluble salts in acid medium.

In basic medium, reduction reactions were observed at all temperatures (Fig. S3), these results are in accordance with the literature [25]. Molybdates have a strong interaction in alkaline mediums and can form different salts of molybdenum (VI) as molybdate (MnO_4^{2-}) and molybdenum oxide (MnO_3) depending on the alkalinity of the solution. They also tend to decompose water under these conditions. The reduction of ammonium molybdate can result in the formation of molybdenum hydroxide ($\text{Mo}(\text{OH})_4$) and metallic molybdenum.

Tellurium

The voltammetric profile of the element tellurium was evaluated using TeO_2 both in acidic (Fig. S4) and basic medium (Fig. S5). In acidic medium at 298 K and 313 K, redox reactions were not observed in the potential region investigated. At 333 K a reduction reaction was observed between 0.8 and 1.0 V, which can be attributed to the reduction of this compound to elemental Te [26], according to the reaction below (Eq. (6)):



Voltammetric analysis of tellurium dioxide at pH 8 reveals the presence of two cathodic peaks, which occurred in all concentrations and temperatures studied. The dissolution of TeO_2 rises in alkaline buffer when compared to acid buffer medium; this phenomenon can be attributed to the formation of TeO_3^{2-} and HTeO_3^- species which could be easily reduced mostly obtaining elemental Te [25, 27]. The cyclic voltammetry results of TeO_2 at pH 5 and 333 K show that the increase in temperature resulted in a reduction reaction. These findings contrast with the experiments conducted at 298 and 313 K (Fig. S5) where no faradaic peaks were detected. Considering that the same behavior occurred with ruthenium at the same temperature it is possible to expect a decrease in the yield of iodine separated under these conditions.

Effect of interferents on iodine redox processes

The effect of the possible interferents (Mo, Ru, and Te) was investigated in both acidic and basic media. Firstly, each voltammogram obtained by iodine and interferent species individually, at pH 5, concentration of 0.010 mol.L^{-1} , and at 298, 313, and 333 K, was plotted in Fig. 3a, c, and e. Then, these voltammograms were compared to others obtained under the same parameters but with all the species in the same solution in concentrations of 0.001, 0.005, and 0.010 mol L^{-1} (Fig. 3b, d, and f). Finally, the voltammograms obtained in basic media are presented in the Supplementary Material, Fig. S6, only for comparison.

The voltammograms of iodine and interferent species in separated solution of pH 5 and temperature of 298 K (Fig. 3a) exhibit only capacitive currents associated with Mo, Ru, and Te. However, when all interferents are present in the same solution and concentration (Fig. 3b) significant differences have been found. In the 0.010 mol L^{-1} solution, the oxidation peak potential that appeared at 0.81 V loses definition in comparison to that observed in Fig. 3a (black curve). Additionally, the reduction potential peak shifts to higher potentials region (0.25 V). In the 0.005 mol L^{-1} an optimal behavior was achieved where is evident that the E_{ap} , corresponding to the oxidation of iodide to form iodine, remains consistent with minimal transformation compared to the voltammogram of the individual specie. A decrease in the current values of the 0.001 mol L^{-1} concentration compared to the concentrations of 0.01 and 0.005 mol L^{-1} has already been observed when the iodide was analyzed individually (see Fig. 2). Now, with the addition of the interferent species, the peaks exhibit a loss of definition (see Fig. 3b). It is plausible that these results can be attributed to the redox reactions of the interfering species, which may hinder the separation of iodine with high yield.

Increasing the temperature to 313 K (Fig. 3d, compared to 3c), the iodine peaks were well defined and easily identifiable at concentrations of $0.005 \text{ mol. L}^{-1}$, but not at 0.010 and 0.001 mol L^{-1} . In the concentration of 0.001 mol L^{-1} , the poorly defined iodine peak, as mentioned before, may indicate the presence of interfering reactions which becomes more prominent due to, at this concentration, iodine peaks are obtained with low current values. In the case of 0.01 mol L^{-1} , only a broad reduction peak potential was observed at 0.34 V, while the oxidation peak potential loses definition.

The most contrasting finding at pH 5 occurred at 333 K (Fig. 3f). At these conditions, the oxidation of iodine was not detected at concentrations of 0.001 mol L^{-1} and $0.005 \text{ mol. L}^{-1}$, nor were any other redox processes related to interfering species identified. At a concentration of 0.01 mol L^{-1} , there was a noticeable increase in the cathodic current, which is consistent with previous voltammograms that indicated ruthenium redox reaction $\text{Ru}^{3+}/\text{Ru}^{2+}$ at 0.9 V vs.

Ag/AgCl (Supplementary Material, Fig. S2), as well as tellurium redox $\text{Te}^{4+}/\text{Te}^0$ between 0.8 and 1.0 V vs. Ag/AgCl (Supplementary Material, Fig. S4) under these conditions.

Iodine capture and quantitative iodine analysis

After the cyclic voltammetry experiments, the optimal potential for iodine separation was determined to be 0.81 V. Despite minor variations in the oxidation peak potential, this potential value ensures the occurrence of iodide oxidation to iodine. Thus, the separations were conducted using two distinct methods: (i) single potential step and (ii) square wave form as described previously. In the collector, with the presence of $\text{KOH } 0.1 \text{ mol L}^{-1}$, a color change from colorless to yellow was observed, indicating the capture of iodine, followed by the formation of iodide and the formation of I_3^- from the excess of I_2 in the solution, as discussed previously. At 333 K, it was possible to perceive an iodine leakage coming from the cell and from the collector, in addition to the characteristic odor of iodine.

Quantitative analyses after the separation process were more efficient at pH=5 (Table 1) compared to pH=8 (Table 2).

The most significant results were achieved at the temperature of 313 K, especially in less concentrated solutions and square wave potential application. It was found that under these specific conditions, the optimal recovery rate reached 45% from a solution with a concentration of 0.001 mol.L^{-1} . As mentioned in literature review, adsorption and sorption are considered efficient methods to capture iodine, with the potential to recover over 80% of this specie. However, it is important to note that these methods often require a significant amount of time to achieve such high levels of recovery [28]. Additionally, there is a tendency for these methods to experience a rapid decline in performance, resulting in the generation of residues [17].

At the temperature of 298 K, the recovery of iodine decreases when compared to 313 K, under these conditions the method of potential application becomes more significant, as small values of recovery were obtained using potential step method compared to square wave method. Additionally, under these parameters it was possible to recovery iodine from more concentrated solutions.

At 333 K, the lowest iodine separation values were obtained; these results are in agreement with the previous voltammograms, where iodine redox reaction suffer influence from tellurium (Fig. S4) and ruthenium (Fig. S2). Besides that is possible that the iodine leakage verified earlier in the separation step was a factor that contributed to these results.

At pH 8 (Table 2), the quantitative analyses indicated lower recovery when compared to acidic medium. Higher separation values were obtained at lower concentrations at 298 K using the potential step procedure.

At 313 K, iodine separation occurs with poor efficiency. Better results were observed in more concentrated solutions, and there is no significant difference between the values

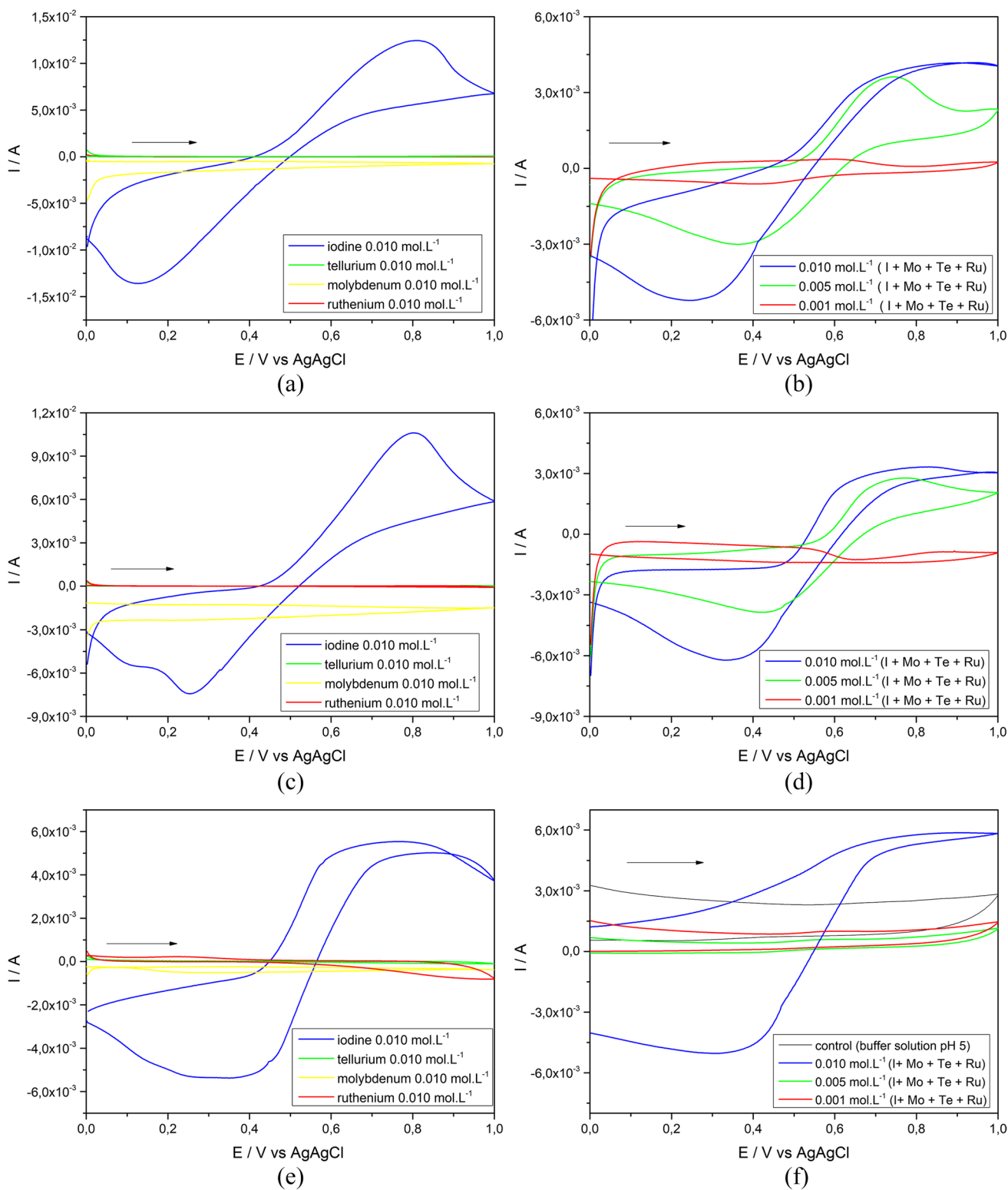


Fig. 3 Plots of the cyclic voltammograms of iodine and interferences (Mo, Te, and Ru), each performed separately, at a concentration of 0.01 mol L^{-1} (a, c, and e). Voltammograms of all elements in the

same solution at concentrations 0.001 , 0.005 , and 0.010 mol L^{-1} (b, d, and f). Experiments at 298 K (a, b); 313 K (c, d); and 333 K (e, f), in acid medium (pH 5)

Table 1 Iodine quantitative analysis in pH=5 at different temperatures

Temperature (K)	Concentration (mol L ⁻¹)	Recovery (%)	
		Square wave	Potential step
298	0.001	13.9	5.6
	0.005	18.6	9.1
	0.01	29.9	12.1
313	0.001	45.2	33.5
	0.005	14.1	17.3
	0.01	13.3	20.1
333	0.001	9.3	13.6
	0.005	3.7	3.8
	0.01	6.1	4.1

Table 2 Iodine quantitative analysis in pH=8 at different temperatures

Temperature (K)	Concentration (mol L ⁻¹)	Recovery (%)	
		Square wave	Potential step
298	0.001	21.4	28.8
	0.005	3.5	8.8
	0.01	7.0	8.1
313	0.001	2.3	1.4
	0.005	5.6	5.8
	0.01	11.2	15.9
333	0.001	1.2	1.2
	0.005	5.6	1.4
	0.01	3.3	9.8

obtained in square wave or potential step application. At 333 K, low values of efficiency in the separation of iodine were obtained, because of the difficulty in resolubilizing iodine at elevated temperature. These findings are in contradiction with the literature since it is already known that iodine solubility increases with the increase in temperature. Additionally, an increase in solubility occurs when the KI is already present in the solution because of the formation of water-soluble triiodide ions, as mentioned in literature review. However, aqueous solutions of iodine are unstable and may contain various ions (HOI, OI⁻, HI₂O⁻, I₂O⁻), which formation are dependent of pH or temperature, that could interfere in the solubility [29]. Thus, it is possible that some of these ions were formed in the collector, decreasing the solubility and hindering the iodine separation.

Conclusions

In this work, the optimized conditions for iodine electrochemical separation have been studied. The voltammetry results for the behavior of iodine in the absence of interferents indicate

that the iodine redox process can be better identified at temperatures of 298 K and 313 K with better definition of the oxidation and reduction peak potentials at the highest concentrations 0.010 and 0.005 mol.L⁻¹. The identified potential values are around 0.8 V vs. Ag/AgCl, which corresponds to the standard iodine oxidation reaction potential (0.535 vs. SHE). Additionally, in the acidic solution, peak current values can be observed that increase with the concentration of the potassium iodide solution. Comparing the voltammograms obtained at 298 K and 313 K, it is possible to notice that the redox processes occurring at higher negative potentials are quite different, but there were no significant changes in the region where the iodide oxidation occurs (Fig. 2a, b). At 333 K (Fig. 2c), a decrease in the current density can be observed when compared to the lower temperatures, and there is a loss in the definition of the redox processes under study. Comparing the voltammograms in the potential region where occur the redox process of iodine in the presence of interferents in separated solutions, significant currents associated with Mo, Ru, or Te redox processes cannot be observed. However, when all interferents are in the same solution, there is a loss of definition regarding the iodide oxidation process for all temperatures evaluated and at the highest and lowest concentrations of KI. In the 0.005 mol L⁻¹ solution, on the other hand, the oxidation peak potentials are similarly defined in both situations. In addition, at lower concentration of 0.001 mol L⁻¹ and higher temperature all redox process loses definition.

Finally, higher iodine recoveries were obtained in acidic medium (pH 5 buffer solution). In this condition, the best temperature for the separation was 313 K. The recoveries of iodine in basic medium were lower than those obtained in acidic medium.

Supplementary Information The online version contains supplementary material available at <https://doi.org/10.1007/s10008-024-06062-7>

Acknowledgements The authors would like to thank the Coordination for the Improvement of Higher Education Personnel (CAPES).

Author contribution Thayna Campeol Marinho: writing, investigation, methodology, and formal analysis. Elita Fontenele Urano de Carvalho: funding acquisition. Valéria Cristina Fernandes: conceptualization, methodology, writing, and revision. Artur José Santos Mascarenhas: writing and revision. Elisabete Inácio Santiago: supervision, review, conceptualization, and funding acquisition.

Funding Coordenação de Aperfeiçoamento de Pessoal de Nível Superior

Declarations

Competing interests The authors declare no competing interests.

References

- International Atomic Energy Agency (2016). "Diagnostic radiopharmaceuticals, radioactive drugs for diagnosis | IAEA." Iaea.org. April 13, 2016. <https://www.iaea.org/topics/diagnostic-radiopharmaceuticals>
- Iodine-131 (^{131}I) Who discovered iodine? (2003). Available at: https://doh.wa.gov/sites/default/files/legacy/Documents/Pubs/320-085_i131_fs.pdf?uid=62f9bbec6997d
- Flux G, Leek F, Gape P, Gear J, Taprogge J (2022) Iodine-131 and iodine-131-meta-iodobenzylguanidine dosimetry in cancer therapy. *Semin Nucl Med* 52(2):167–177. <https://doi.org/10.1053/j.semnuclmed.2021.11.002>
- Van Nostrand D, Wartofsky L (2007) Radioiodine in the treatment of thyroid cancer. *Endocrinol Metab Clin North Am* 36(3):807–822. <https://doi.org/10.1016/j.ecl.2007.04.006>
- El-Azony KM, Mohty AA, Salah M (2004) Separation and purification of ^{131}I from tellurium material using ion exchange for preparing tetra-butyl ammonium iodide (^{131}I). *Appl Radiat Isot* 61(6):1185–1188. <https://doi.org/10.1016/j.apradiso.2004.04.015>
- Wioletta W (2010) Studies on separation and purification of ^{99}Mo from Nat-U, ^{131}I and ^{103}Ru . *Nucl Med Biol* 37(6):715–15. <https://doi.org/10.1016/j.nucmedbio.2010.04.127>
- Rao A, Sharma AK, Pradeep Kumar MM, Charyulu BST, Ramakumar KL (2014) Studies on separation and purification of fission ^{99}Mo from neutron activated uranium aluminum alloy. *Appl Radiat Isot* 89(July):186–191. <https://doi.org/10.1016/j.apradiso.2014.02.013>
- Nazari K, Mohammad Ghannadi-Maragheh M, Shamsaii, and H. Khalafi, (2001) A new method for separation of ^{131}I , produced by irradiation of natural uranium. *Appl Radiat Isot* 55(5):605–608. [https://doi.org/10.1016/s0969-8043\(01\)00111-7](https://doi.org/10.1016/s0969-8043(01)00111-7)
- Chatopadhyay S, Das S (2009) A simple and rapid technique for radiochemical separation of iodine radionuclides from irradiated tellurium using an activated charcoal column. *Appl Radiat Isot* 67(10):1748–1750. <https://doi.org/10.1016/j.apradiso.2009.03.114>
- El-Absy MA, Aly HF, Mousa MA, Mostafa M (2004) Sequential distillation of fission-produced radioiodine and radiouranium from sulfuric acid solutions. *J Radioanal Nucl Chem* 261(1):163–172. <https://doi.org/10.1023/b:jrnsc.0000030951.39488.64>
- Kim T-W, Seung-Kon L, Suseung L, Jun Yeob L, Sang-Wook K (2017) Development of silver nanoparticle-doped adsorbents for the separation and recovery of radioactive iodine from alkaline solutions. *Appl Rad Iso* 129(November):215–21. <https://doi.org/10.1016/j.apradiso.2017.07.033>
- Chatopadhyay S, Das SS (2010) Recovery of ^{131}I from alkaline solution of N-irradiated tellurium target using a tiny Dowex-1 column. *Appl Radiat Isot* 68(10):1967–1969. <https://doi.org/10.1016/j.apradiso.2010.04.033>
- El-Absy MA, El-Garhy MA, El-Amir MA, Fasih TW, El-Shahat MF (2010) Separation and purification of ^{131}I from neutron irradiated tellurium dioxide targets by wet-distillation method. *Sep Purif Technol* 71(1):1–12. <https://doi.org/10.1016/j.seppur.2009.06.008>
- Treushchenko NN, Dmitrievskii BA, Kazakov AA, Tsvetkov SK, Popov AY, Galkin BY, Treushchenko VA (2010) Recovery and long-term storage of radioactive iodine using magnesium-containing composites. *Theor Found Chem Eng* 44(4):587–591. <https://doi.org/10.1134/s004057951004041x>
- Yang D, Liu H, Liu L, Sarina S, Zheng Z, Zhu H (2013) Silver oxide nanocrystals anchored on titanate nanotubes and nanofibers: promising candidates for entrapment of radioactive iodine anions. *Nanoscale* 5(22):11011. <https://doi.org/10.1039/c3nr02412a>
- Damasceno Marcos O, Tatiana S, Balogh Christina ALG, De Forbicini O, International Nuclear atlantic Conference (2018) Recovery of ^{131}I from fission ^{99}Mo production process by distillation method. *Repositorio.ipen.br*, January. <http://repositorio.ipen.br/handle/123456789/28307>
- Mateo DR, Marina V, Santiago Q, Gemma TP, Laura F, Carlos PC (2021) Silver-functionalized UiO-66 metal-organic framework-coated 3D printed device for the removal of radioactive iodine from wastewaters. *Appl Mater Today* 24(September):101130. <https://doi.org/10.1016/j.apmt.2021.101130>
- Dale GE, Dalmas DA, Gallegos M, Jackman KR, Kelsey CA, May I, Reilly SD, Stange GM (2012) ^{99}Mo separation from high-concentration irradiated uranium nitrate and uranium sulfate solutions. *Ind Eng Chem Res* 51(40):13319–13322. <https://doi.org/10.1021/ie3008743>
- Röttcher NC, Yu-Ping Ku, Minichova M, Ehelebe K, Cherevko S (2023) Comparison of methods to determine electrocatalysts' surface area in gas diffusion electrode setups: a case study on Pt/c and PtRu/C. *Journal of Physics: Energy* 5(2):024007. <https://doi.org/10.1088/2515-7655/acbe1b>
- Carter RN, Kocha SS, Wagner F, Fay M, Gasteiger HA (2007) Artifacts in measuring electrode catalyst area of fuel cells through cyclic voltammetry. *ECS Trans* 11(1):403–410. <https://doi.org/10.1149/1.2780954>
- Elgrishi N, Rountree KJ, McCarthy BD, Rountree ES, Eisenhart TT, Dempsey JL (2017) A practical beginner's guide to cyclic voltammetry. *J Chem Educ* 95(2):197–206. <https://doi.org/10.1021/acs.jchemed.7b00361>
- Evans DH, O'Connell KM, Petersen RA, Kelly MJ (1983) Cyclic voltammetry. *J Chem Educ* 60(4):290. <https://doi.org/10.1021/ed060p290>
- Kolthoff IM, Jordan J (1953) Voltammetry of iodine and iodide at rotated platinum wire electrodes. *J Am Chem Soc* 75(7):1571–1575. <https://doi.org/10.1021/ja01103a015>
- Silva PP, Guerra W (2011) Rutênio. *Química Nova na Escola* 34(2):99–100. http://qnesc.sbq.org.br/online/qnesc34_2/08-EQ-07-11.pdf
- Pourbaix M (1974) Atlas of electrochemical equilibria in aqueous solutions. *Natl Assoc Corrosion Eng*
- Rudnik E, Sobesto J (2011) Cyclic voltammetric studies of tellurium in diluted HNO_3 solutions. *Arch Metall Mater* 56(2):270–277. <https://doi.org/10.2478/v10172-011-0030-z>
- Ba LA Mandy D, Vincent J, Claus J (2010) Tellurium: an element with great biological potency and potential. *Organic Biomol Chem* 8(19):4203. <https://doi.org/10.1039/c0ob00086h>
- Asmussen RM, Matyáš J, Qafoku NP, Kruger AA (2019) Silver-functionalized silica aerogels and their application in the removal of iodine from aqueous environments. *J Hazard Mater* 379(November):119364. <https://doi.org/10.1016/j.jhazmat.2018.04.081>
- Makhayeva DN, Irmukhametova GS, Khutoryanskiy VV (2020) Polymeric iodophors: preparation, properties, and biomedical applications. *Rev J Chem* 10(1–2):40–57. <https://doi.org/10.1134/s2079978020010033>

Publisher's Note Springer Nature remains neutral with regard to jurisdictional claims in published maps and institutional affiliations.

Springer Nature or its licensor (e.g. a society or other partner) holds exclusive rights to this article under a publishing agreement with the author(s) or other rightsholder(s); author self-archiving of the accepted manuscript version of this article is solely governed by the terms of such publishing agreement and applicable law.